Detecting leaks in gas-filled pressure vessels using acoustic resonances

K. A. Gillis[1], M. R. Moldover[1], and J. B. Mehl[2]

[1] Sensor Science Division, National Institute of Standards and Technology, Gaithersburg, MD, 20899-8360 USA
[2] 36 Zunuqua Trail, PO Box 307 Orcas, WA 98280-0307, USA

E-mail: keith.gillis@nist.gov

Abstract

We demonstrate that a leak from a large, unthermostatted pressure vessel into ambient air can be detected an order of magnitude more effectively by measuring the time dependence of the ratio p/f^2 than by measuring the ratio p/T. Here f is the resonance frequency of an acoustic mode of the gas inside the pressure vessel; p is the pressure of the gas, and T is the kelvin temperature measured at one point in the gas. In general, the resonance frequencies are determined by a mode-dependent, weighted average of the square of the speed-of-sound throughout the volume of the gas. However, the weighting usually has a weak dependence on likely temperature gradients in the gas inside a large pressure vessel. Using the ratio p/f^2, we measured a gas leak $(\mathrm{d}M/\mathrm{d}t)/M \approx -1.3\times10^{-5}\ \mathrm{h}^{-1} = 0.11\ \mathrm{year}^{-1}$ from a 300-liter pressure vessel filled with argon at 450 kPa that was exposed to sunshine-driven temperature and pressure fluctuations as large as $(\mathrm{d}T/\mathrm{d}t)/T \approx (\mathrm{d}p/\mathrm{d}t)/p \approx 5\times10^{-2}\ \mathrm{h}^{-1}$ using a 24-hour data record. This leak could not be detected in a 72-hour record of p/T. (Here M is the mass of the gas in the vessel and t is time.)

Keywords: leak, leak detection, pressure vessel, acoustic resonance, resonance frequency

Introduction

In a gas, the speed of sound u is a known function of temperature. The time for a free-traveling sound wave to propagate a distance is determined by an average temperature of the gas along the traveled path. Likewise, the frequency of an acoustic resonance in a closed cavity is determined by a mode-dependent average of temperature over the volume of the cavity. Conversely, the average temperature of a gas in a cavity can be deduced from measurements of the frequencies of gas resonances [1,2].

Previously, in the context of gas flow standards, we have shown that the mass M of gas within a pressure vessel ("tank") may be deduced from measurements of the gas pressure and the frequencies of the microwave and acoustic resonances within the tank [3,4]. The microwave frequencies determined the shape and volume of the tank. The acoustic measurements eliminated the need for multiple thermometers to obtain an average temperature with sufficient accuracy for flow metrology. Acoustic measurements are advantageous when it is impractical to install many calibrated thermometers throughout a large, gas-filled volume. Using this technique, we also showed that the apparent value of M did not change when we imposed a time-independent temperature gradient such that the gas in a tank was heated on the top and cooled on the bottom as shown in Fig. 12 of Ref. [4]. The time-independent temperature gradient simulated the gradient that resulted from a gas flowing through a meter being calibrated and then into a large collection vessel [5]. During this earlier work [4], the tank's temperature was well-controlled. We noticed that the gas pressure decreased slowly, and we attributed the decrease to a leak from the tank into the ambient air. The leak was an unavoidable nuisance; therefore, the data in Ref. [4] were corrected to account for the leak. In this work, we show that the leak could have been detected easily, even in the presence of large temperature fluctuations, by measuring the decrease of the ratio p/f^2 with time. Here f is the resonance frequency of an acoustic mode of the gas inside the pressure vessel; p is the pressure of the gas, and T is the kelvin temperature measured at one point in the gas. To first order, the resonance frequencies are determined by a mode-dependent, weighted average of the square of the speed-of-sound u throughout the volume of the gas, *i.e.* $f^2 \propto \langle u^2 \rangle$, where

$$\langle u^2 \rangle = \frac{\int_V u^2 |\varphi|^2 \, dV}{\int_V |\varphi|^2 \, dV} \, . \tag{1}$$

The acoustic velocity potential φ is proportional to the local acoustic pressure in the standing wave when the temperature is uniform. Regions where $\varphi = 0$, *i.e.* pressure nodes, do not contribute to the weighted average. The weighted average in Eq. (1) has a weak dependence on temperature gradients that are likely to form in the gas inside a large pressure vessel.

In this work, we placed the 0.3 m^3 gas-filled (argon at 0.45 MPa) tank from Ref. [4] in direct sunlight that generated time-dependent temperature and pressure variations in the gas as large as $(dT/dt)/T \approx (dp/dt)/p \approx 5\times10^{-2}\ h^{-1}$. (Here, "$t$" denotes time and T is the kelvin temperature measured at one location in the gas.) The sunlight-driven variations obscured a gas leak of $(dM/dt)/M \approx -1.3\times10^{-5}\ h^{-1}$ out of the tank into ambient air, even when the pressure data were averaged over 3 days. However, the leak rate was deduced with an uncertainty of about ±30 % from measurements of p/f^2 averaged over just 1 day, where f is the resonance frequency of a single acoustic mode. (Throughout this paper, we report the statistical, standard uncertainty corresponding to a 68 % confidence level.) Thus, measurements of the pressure and a resonance frequency can efficiently detect a leak from large, unthermostatted volumes, such as an air lock, or a vessel designed to contain a hazardous process gas, or a tank used to store liquids and/or gases outdoors, or a large subterranean cavern with distinct resonances.

Figure 1. 300-liter compressed-air tank on a pallet outside a NIST laboratory.

Acoustic Resonances and the Mass of Gas in an Isothermal Cavity.

In this section, we show that the ratio p/f^2 is proportional to the mass M of the gas in a tank when temperature of the gas is uniform. Therefore, a leak that generates negative values of dM/dt can be detected by measuring a decrease of p/f^2 with time.

The molar density ρ_m of the gas in a tank is related to the pressure p and the speed of sound u in the gas by combining the virial equation of state

$$p = \rho_m RT(1 + B\rho_m + \ldots) \qquad (2)$$

with the analogous equation [6] for the square of the speed of sound

$$u^2 = \frac{\gamma_0 RT}{M_\mathrm{m}}\left(1 + \frac{\beta_\mathrm{a} p}{RT} + \ldots\right) \quad . \tag{3}$$

We then obtain an expression for the mass $M = \rho_\mathrm{m} M_\mathrm{m} V_\mathrm{tank}$ of the gas in the tank

$$M = \frac{\gamma_0 p V_\mathrm{tank}}{u^2}\left[1 + (\beta_\mathrm{a} - B)\frac{p}{RT} + \ldots\right] , \tag{4}$$

In Eqs. (2) through (4), M_m is the average molar mass of the gas; V_tank is the volume of the tank; R is the universal gas constant; $\gamma_0 \equiv C_p/C_V$ is the gas's zero-pressure heat-capacity ratio; and, β_a and B are the gas's acoustic and the density second virial coefficients, respectively.

The speed of sound u in the gas inside the tank is well-approximated by $u = f_N L_N$ where f_N is the resonance frequency of the acoustic mode of the gas identified by the subscript N, and L_N is a characteristic length that depends upon the mode N. For cavities with special geometries (*e.g.* right circular cylinder, sphere, ...), L_N can be calculated analytically. For tanks with complicated shapes (such as the tank in Fig. 1), L_N can be accurately calculated using numerical methods, provided that the shape of the tank is known or is fitted to microwave resonance frequency measurements [4]. For a tank that does not contain obstructions and has rigid, non-porous walls, the fractional corrections to $u = f_N L_N$ are on the order of g_N/f_N, where g_N is the half-width of the acoustic resonance with frequency f_N. Throughout the range of the present measurements, $g_N/f_N \approx 3\times10^{-4}$ and changes in g_N/f_N are less than 10^{-5}; therefore, we ignored corrections resulting from g_N/f_N. We also ignored the small change of V_tank that occurred when the pressure varied by approximately 8 % in the range 427 kPa < p < 463 kPa.

In this work, we are concerned with detecting small *changes* in M resulting from a leak; therefore, accurate values of L_N and V_tank are unnecessary. However, our sensitivity to detect small leaks in the presence of large temperature changes is improved by approximately a factor of two if we account for the thermal expansion of L_N and V_tank by using the expressions $L_N = L_{N,0}[1 + \alpha_\mathrm{T}(T_\mathrm{tank} - T_0)]$ and $V_\mathrm{tank} = V_\mathrm{tank,0}[1 + 3\alpha_\mathrm{T}(T_\mathrm{tank} - T_0)]$. Here T_tank is the average temperature indicated by two thermistors attached to the top and bottom of tank; T_0 is an

arbitrary reference temperature and α_T is the coefficient of linear thermal expansion of the metal comprising the tank. (For T_0 we used the first value of T in a series of measurements and we used $\alpha_T = 11.7\times10^{-6}$ K^{-1} from [3].) Substituting $u = f_N L_N$ and the above expressions for L_N and V_{tank} into Eq. (4), the thermal expansion correction is $[1+3\alpha_T(T_{tank}-T_0)]/[1+\alpha_T(T_{tank}-T_0)]^2 \approx 1+\alpha_T(T_{tank}-T_0)$, to first order, assuming the expansion is isotropic. The small term $(\beta_a - B)p/(RT)$ in Eq. (4) contains the difficult-to-measure average gas temperature T. It is convenient to eliminate T by using the approximation $T/T_1 \approx (f_N/f_{N,1})^2$, where $f_{N,1}$ is the acoustic resonance frequency at the temperature T_1. During the night, there were no heat sources (*e.g.* sunlight) on our tank; therefore, the average temperature of the tank's wall and the average temperature of the gas approached a common value: $T_{tank} \approx T \equiv T_1$. This expectation is consistent with the near agreement (±0.4 K) between temperature sensors that we had taped to points on of the top and bottom surfaces of the tank. Therefore, at night the small correction term $(\beta_a - B)p/(RT)$ can be accurately evaluated using frequency measurements as a surrogate for the gas temperature.

After accounting for the thermal expansion and for measuring a frequency instead of measuring the speed of sound, Eq. (4) becomes:

$$M_{p/f^2,c} = \frac{\gamma_0 V_{tank,0}}{L_{N,0}^2}\frac{p}{f_N^2}\left[1+\alpha_T(T_{tank}-T_0)+(\beta_a - B)\frac{p}{RT_1}\frac{f_{N,1}^2}{f_N^2}\right], \quad (5)$$

where we have neglected higher-order terms and introduced the subscript "$p/f^2,c$" to emphasize that this calculation of M depends upon frequency measurements and includes the correction terms in square brackets.

For many common gases including dry air, accurate values of the temperature-dependent quantities γ_0, β_a and B are available in a user-friendly database [7]. In this work, the gas temperature ranged from 20 °C to 45 °C; a typical pressure was 450 kPa; and, the test gas was argon for which $\gamma_0 \equiv 5/3$. Under these limited conditions, the virial coefficient term in square brackets in Eq. (5) changes by only 1/4 as much as the changes in the thermal expansion term. Specifically, when the temperature increases from 20 °C to 45 °C, the term $(\beta_a - B)p/(RT)$

increases by 0.000068 (from 0.004707 to 0.004775) [7]. In the same range, $\alpha_T(T-T_0)$ increases by 0.00029. If we had used dry air instead of argon, the change in the virial coefficient term in Eq. (5) would be 78 % of the change in the thermal expansion term.

Conventionally, leaks from large tanks are detected without measuring acoustic resonance frequencies. For example, one could monitor the gas pressure to detect a leak. This approach is greatly improved by monitoring the ratio p/T, where T is the temperature of the gas measured at some point inside the tank. Similar to the acoustic method, monitoring the pressure can be refined by accounting for the thermal expansion of V_{tank} and accounting for the virial corrections to the ideal gas law. With these refinements, an expression for the mass of gas in a tank as a function of the measured temperature and pressure is:

$$M_{p/T,c} = \frac{V_{\text{tank},0} M_{\text{m}}}{R} \frac{p}{T} \left[1 + 3\alpha_T (T_{\text{tank}} - T_0) - B \frac{p}{RT} + \cdots \right], \tag{6}$$

where the symbol $M_{p/T,c}$ emphasizes that this calculation of the mass of gas in the tank depends upon the ratio p/T and includes corrections to the same order as Eq. (5). The complexity of Eq. (6) is comparable to that of Eq. (5). However, at each level of complexity, $M_{p/f^2,c}$ computed by Eq. (5) leads to more sensitive leak detection than $M_{p/T,c}$ computed from Eq. (6).

Resonance Frequencies are Insensitive to Linear Temperature Gradient

We expected that measurements of p/f^2 would be useful because of the remarkable prediction that a linear temperature gradient (such as the gradients illustrated in Fig. 2) will change the resonance frequencies f_N by a fraction proportional to the square of the gradient, provided that the gradient is not too large [4]. In this work, we detected sun-generated, vertical temperature differences as large as $\Delta T \equiv (T_{\text{top}} - T_{\text{bottom}})$ =15 K near the average temperature T_{ave} = 300 K. If this measured temperature difference occurred when the temperature was a time-independent, linear function of depth in the tank, the predicted frequency shifts are $\Delta f_N / f_N \propto \left[\Delta T / (2T_{\text{ave}})\right]^2$ $\approx 6\times10^{-4}$. Because the measured values of $\Delta f_N/f_N$ were smaller than 6×10^{-4}, we speculate that ΔT < 15 K inside most of the tank.

Stated more formally, Gillis *et al*. calculated the effects of a temperature gradient on the acoustic resonance frequencies of a model "tank" that was a right circular cylindrical cavity (with inner radius a, length L, and interior volume V) oriented with its symmetry axis horizontal [4]. Their model cavity was filled with a compressible, thermally conducting fluid that supported sound waves but was otherwise stationary (*i.e.* no convection). The cylindrical shell was mechanically rigid, and its position was fixed in space. The shell was not isothermal; its temperature $T_w(a,\theta,z)$ was a specified function of position. (The z-axis is oriented horizontally along the cylinder's symmetry axis.) The steady-state temperature $T(\mathbf{r})$ of the gas in the cavity was expressed as $T(\mathbf{r}) = T_0\left[1+\tilde{\tau}_0\mathcal{T}(\mathbf{r})\right]$, where T_0 is the average gas temperature over the cavity volume; $\tilde{\tau}_0$ is a dimensionless scale factor much smaller than 1; and the profile function $\mathcal{T}(\mathbf{r})$ is determined from the Laplace equation $\nabla^2\mathcal{T} = 0$, subject to the Dirichlet boundary condition $\tilde{\tau}_0\mathcal{T}(a,\theta,z) = \left[T_w(a,\theta,z) - T_0\right]/T_0$ at the wall. They used first-order perturbation theory to solve the Helmholtz equation with a spatially varying speed of sound $u^2 = u_0^2\left[1+\tilde{\tau}_0\mathcal{T}(\mathbf{r})\right]$ and compared the resonance frequencies of the gas with and without the small perturbation $\tilde{\tau}_0\mathcal{T}(\mathbf{r})$. For a gas-filled cylindrical cavity containing no heat sources or sinks, they concluded that if $\mathcal{T}(\mathbf{r})$ is a linear function of distance, then the acoustic resonance frequency for any mode depends upon $\tilde{\tau}_0^2$, but not upon $\tilde{\tau}_0$ provided that $\mathcal{T}(\mathbf{r})$ is a solution to the Laplace equation and $\langle\mathcal{T}\rangle = 0$. This result is intuitive because a standing wave in the cavity may be decomposed into counter-propagating traveling waves, whose round-trip travel times through a linear temperature gradient will be the same and unchanged from the uniform case to first order.

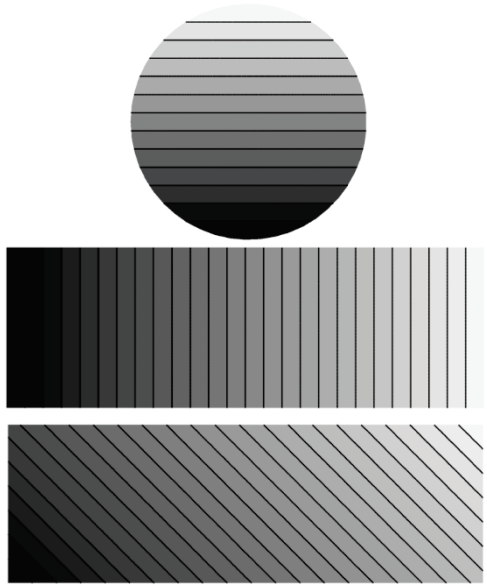

Figure 2. Three examples of linear temperature gradients in a stationary fluid inside a cylindrical tank with a horizontal cylinder axis. Dark shades indicate temperatures below the average; light shades indicate temperatures above the average. The equally-spaced lines represent isotherms. Top: vertical cross-section with a vertical gradient. Center: horizontal cross-section with an axial gradient. Bottom: a superposition of horizontal and vertical linear temperature gradients produces a linear temperature gradient with diagonal isotherms. In a real fluid, buoyancy makes the center and bottom configurations unstable.

Description of the Tank

The tank was a pressure vessel that was commercially manufactured for use as an air receiver with a maximum operating pressure of 1.38 MPa (Silvan Industries[1], Inc., Marinette, WI, USA, Part Number A10031). The manufacturer stated that it was designed and built to comply with ASME Code, Section VIII, Div. 1, 20th Edition. As shown in Fig. 1, the tank was a horizontal, approximately circular cylinder with hemispheroidal "heads" welded to each end of the cylinder. The cylindrical section had a length of 1.34 m, an internal diameter of 0.50 m, and a wall thickness of 3.9 mm. The heads were approximately oblate hemispheroids (that is, half of an ellipse of revolution) with a 0.12 m semi-minor axis and a 3.2 mm wall thickness. We did not modify the tank for this research. Additional details can be found in [4].

Seven ports penetrated the tank's walls. At each port, the manufacturer had welded a threaded fitting to the outside of the tank. The manufacturer provided threaded caps that matched each port. Before sealing the caps to the ports, we re-tapped all the threads and wrapped the male threads with polytetrafluoroethylene (PTFE) tape. We detected leaks through these threaded seals by painting them with soapy water and looking for bubbles. We reduced the leaks by tightening the seals until bubbles were no longer observed. As shown below, the tank continued to leak at an average rate $(\mathrm{d}M/\mathrm{d}t)/M \approx -1.3\times10^{-5}\ \mathrm{h}^{-1}$ which corresponds to a bubble rate of approximately 1 mm^3/s. This residual appeared to increase slightly during the 3 days of measurements. See Fig. 3(E). A month after the data in Fig. 3 were acquired, the leak had increased to $-2.4\times10^{-5}\ \mathrm{h}^{-1}$.

The leak rate reported here is within a factor of 2 of the leak rate reported in Ref. [4], when the data from the earlier work are adjusted for the higher pressure (600 kPa) used at that time. This is remarkable because the interval between the data sets was one year during which the tank had been moved and several seals had been replaced.

Materials, Instruments, and Measurements

[1] In order to describe materials and procedures adequately, it is occasionally necessary to identify commercial products by manufacturers' name or label. In no instance does such identification imply endorsement by the National Institute of Standards and Technology, nor does it imply that the particular product or equipment is necessarily the best available for the purpose.

Because the thermophysical properties of argon are accurately known [7], we used technical grade argon (molar fraction of argon = 99.996 %) as the test gas.

We used a calibrated thermometer-probe to measure the temperature of the gas T_{probe} at a single point inside the tank. The probe passed through a hermetic seal in one of the manufacturer's ports and was sensitive to the temperature approximately 1 cm below the top surface of the tank. Two thermistors were taped to the outside of the tank and covered with aluminum foil. One thermistor indicated T_{top}, the temperature of the metal at one point on the top of the tank; the second thermistor indicated T_{bottom}. The read-out electronics for this thermometer-probe and for both the thermistors were located in an air-conditioned laboratory. The pressure gauge was also located in the laboratory; a tube connected the gauge to a fitting that had been soldered into one of the ports in the tank. The data in Fig. 3 span the pressure range 426.7 kPa < p < 462.7 kPa and the temperature range 20.8 °C < T_{probe} < 45.3 °C.

The acoustic resonances in the gas were driven using a home-made acoustic source and detected using a home-made acoustic detector, described in [4]. These transducers were built into pipe fittings that were screwed into the ports located near the ends of the top surface of the tank. Because the tank was unthermostatted and exposed to time-dependent heating by the sun, the drifting resonance frequency could not be determined from a carefully measured resonance line shape. Fortunately, the resonance line shape is unnecessary to detect and quantify a leak from a large tank. Instead, we tracked the resonance frequency using a computer-controlled PID (proportional-integral-differential) algorithm and the quadrature component of the microphone signal, measured with a lock-in amplifier, as a null detector. The phase of the lock-in was set beforehand so that the quadrature signal was zero at the resonance frequency. The lock-in time constant was 30 ms. Our frequency-tracking method used sophisticated, expensive laboratory instruments, but more economical yet effective methods exist. For example, it should be possible to detect leaks using an acoustic resonance in the gas as the frequency-determining element of an oscillator and measuring the oscillator's frequency (or period) with a counter-timer.[8,9]

At intervals of 3 s, we measured the frequency of the 2nd longitudinal acoustic resonance of the gas in the tank $f_{(2,0,0)}$. (We follow Ref. [4] in using the subscript (2,0,0) to identify the acoustic

resonance of the argon-filled tank with a corresponding mode of a perfect, closed, right circular cylindrical cavity.) In a perfect cylindrical cavity, the (2,0,0) gas oscillations are parallel to the cylinder's axis and form a standing wave whose pressure nodes and antinodes are planes perpendicular to the axis: an antinode at each end, an antinode midway between the ends, and a node midway between neighboring antinodes. The gas's center of mass does not move during (2,0,0) gas oscillations. The values of $f_{(2,0,0)}$ for our tank spanned the range 212 Hz < $f_{(2,0,0)}$ < 221 Hz. The half-width of the (2,0,0) mode was $g_{(2,0,0)}$ = 0.067 Hz, and the quality factor[2] $Q_{(2,0,0)} \approx 1600$. In our tank, there were no gas or metal resonance frequencies close enough to $f_{(2,0,0)}$ to interfere with the tracking of $f_{(2,0,0)}$, even while the temperature changed rapidly. The lowest-frequency bending mode of the tank's metal shell occurs near 272 Hz at 295 K and 450 kPa [4]. At lower pressures, this bending mode might have been so close to $f_{(2,0,0)}$ to cause problems. In another test (not shown here), we obtained essentially the same leak rate from measurements of $f_{(1,0,0)}$ the frequency of the 1st longitudinal mode with 105.8 Hz < $f_{(1,0,0)}$ < 110.7 Hz and $g_{(1,0,0)}$ = 0.047 Hz.

Detection of a Leak

Figure 3 displays the time-dependence of the raw data, together with the results of processing the data using increasingly complex algorithms. The record starts at noon on July 31, 2015 and extends for nearly three days. Panel (A) of Fig. 3 displays the fractional pressure deviation from the first pressure measurement (left scale), together with the temperature T_{probe} (right scale). For brevity, we omit the subscript "probe". Each day, between midnight and noon, the pressure and the temperature increased by approximately 8 %. Panel (B) of Fig. 3 displays the time dependence of $\Delta(p/T)/(p/T)_0$, where we use the definition $\Delta(p/T) \equiv (p/T) - (p/T)_0$ and the subscript "0" denotes the first measured value of (p/T). The daily variation of (p/T) is only 1/8 of the daily variations of p and of T; however, this variation is still so large that it obscures the leak.

Panel (C) of Fig. 3 displays the time dependence of the ratio $\Delta M/M_0 = \Delta(p/f^2)/(p/f^2)_0$. Here, we omit the subscript (2,0,0) on f^2. We use the definition $\Delta(p/f^2) \equiv (p/f^2) - (p/f^2)_0$, where the

[2] The quality factor Q of an oscillator is (energy stored) / (energy dissipated per cycle) and refers to the sharpness of the peak in the power spectrum. Q is numerically equal to f / (2g) where f is the center frequency of the resonance peak and 2g is the full width (in frequency) of the peak where the power drops to half of its maximum value.

subscript "0" denotes the first measured value. Note: the vertical scale in Panel (C) is expanded by a factor of 15 compared to the vertical scale in Panel (B). In Panel (C), the slope of the dashed line corresponds to the leak rate $(dM/dt)/M = -1.07\times10^{-5}$ h^{-1}. The root-mean-square (RMS) deviation of $\Delta M/M_0$ from the dashed line is $\sigma_{RMS} = 7.2\times10^{-5}$. These deviations are approximately 0.005× the RMS deviation of p/T from its average value in Panel (B). Thus, replacing T_{probe} with f^2 enabled us to detect the leakage of gas out of the tank, even in the presence of large, sunlight-driven temperature variations.

Panel (D) of Fig. 3 displays the time dependence of the ratio $\Delta M_{p/f^2,c}/M_0$, where the subscript "c" indicates that (p/f^2) is multiplied by the "correction" terms in the square brackets in Eq. (5). The terms account for the thermal expansion of the steel tank and the 2nd virial correction to the ideal-gas equation of state of argon. These corrections increased the apparent leak rate by 16 % to $(dM/dt)/M = -1.24\times10^{-5}$ h^{-1} and reduced the RMS deviation from a linear fit by a factor of 1.6 to $\sigma_{RMS} = 4.4\times10^{-5}$. However, the deviations from the linear fits in Panels (C) and (D) have a daily cycle.

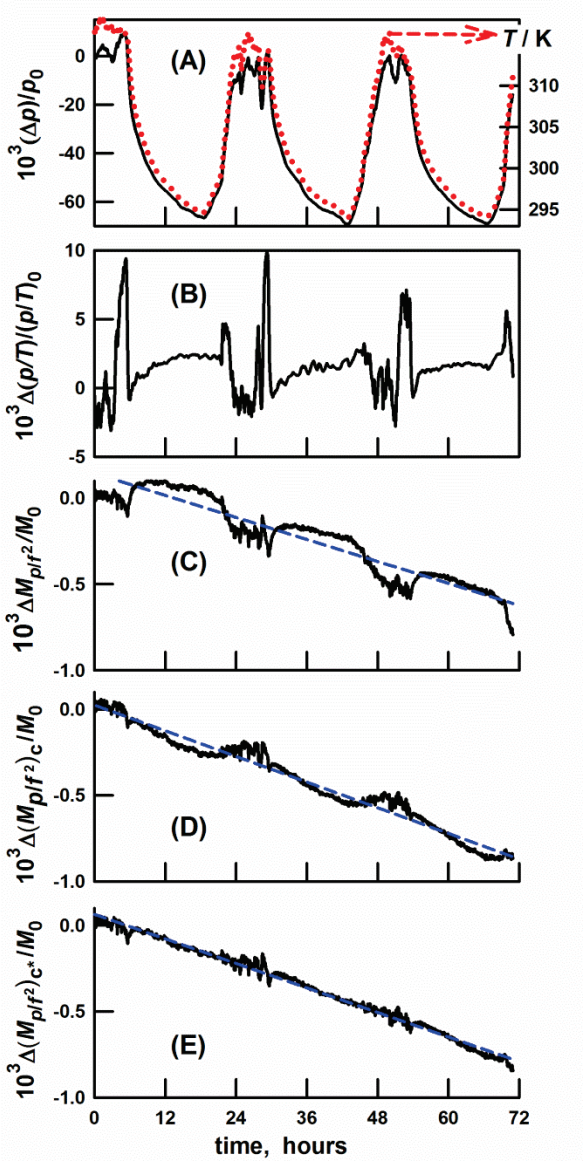

Figure 3. Starting at noon July 31, 2015, the time dependences of: (A) Fractional pressure deviation $(\Delta p)/p_0$ from its initial value (solid curve, left scale) and the kelvin temperature T_{probe} (red dotted curve, right scale). The daily variations of p and T_{probe} are approximately 8 %. (B) Fractional deviation of the ratio (p/T_{probe}) from its initial value $(p/T_{probe})_0$. The daily variation of p/T_{probe} is approximately 1 %. (C) Fractional deviation of $M \propto p/f^2$ from its initial value M_0. (D) Same as (C) except (p/f^2) is corrected to account for the thermal expansion of the tank and non-ideality of argon. (E) Same as (C) except that only 0.6 of the thermal expansion correction is applied. The corrections from (C) to (D) increased the apparent leak rate (*i.e.* slope of the fitted, dashed line) from $(dM/dt)/M = -1.07\times10^{-5}$ h^{-1} to -1.25×10^{-5} h^{-1}. The corrections from (C) to (D) to (E) decreased the RMS deviations from the dashed lines from (7.2 to 4.4 to 2.3)×10^{-5}.

The deviations in Panels (C) and (D) suggest that the corrections applied for the thermal expansion and 2nd virial coefficient have the correct

sign; however, the corrections are too large. In Panel E, we reduced the thermal expansion correction by replacing $\alpha_T(T_{tank}-T_0)$ with $0.6\times\alpha_T(T_{tank}-T_0)$ in Eq. (5). The empirical factor 0.6 eliminated the daily cycle in the deviations from a linear fit and reduced the RMS deviation to $\sigma_{RMS} = 2.3\times10^{-5}$. These improvements might be evidence that the thermal expansion of the tank was not isotropic, as was assumed in the derivation of Eq. (5). Furthermore, the daily temperature variation averaged over the tank's steel surface may have been different than the daily temperature variation averaged over the volume of argon within the tank. In the next section, we speculate about reasons for this.

To summarize, Fig. 3 demonstrates that the ability to detect a leak can be improved by a factor of ≈8 by measuring p/T_{probe} instead of measuring p alone. However, the effectiveness can be improved by a factor of ≈1000 by measuring p/f^2. In hindsight, we speculate that if the temperature probe were located closer to the center of the tank, the advantage of measuring p/T_{probe} over measuring p/f^2 would be smaller. We will test this speculation in future work.

Sunshine-driven temperature gradients and flows

Convection, or buoyancy-driven flow, results from the fundamental coupling between heat transport and fluid motion in a gravitational field. Natural convection inside a container, resulting from a density gradient generated by uneven heating or cooling of the container wall, encompasses a wide range of complicated flow patterns. A horizontal density gradient, *i.e.* normal to the gravity vector, immediately leads to convection. A vertical density gradient with the heavier fluid above is unstable and usually leads to convection. A vertical density gradient with the lighter fluid above leads to stable density stratification. Depending on the conditions, a combination of all of these patterns may be present simultaneously. In this section, we describe the thermal environment of the tank and then try to relate it to some of the results from the literature on convective heat transfer. Our objective is to understand why measuring p/f^2 is so effective in detecting a leak and what might limit its effectiveness. The ideas presented in this section are the subject of ongoing and future research.

To compare our results with the literature, we use the dimensionless temperature difference [the Rayleigh number: $Ra \equiv \beta g \Delta T a^3/(\nu\kappa)$] and the dimensionless ratio (viscous diffusivity)/(thermal

diffusivity) which is the Prandtl number $Pr \equiv \nu/\kappa$. Here, $a = 0.5$ m is the radius of the cylinder and the temperature difference is $\Delta T = T_{\text{hot}} - T_{\text{cold}}$. For our argon-filled tank (300 K, 0.45MPa) we estimated $Ra \approx 4\times10^8$ (ΔT/K) and $Pr = 0.67$ using the thermophysical properties of argon from Ref. [7] and the definitions: $\beta \equiv (\partial V/\partial T)_p/V \equiv$ coefficient of volumetric thermal expansion; $g \equiv$ gravitational acceleration; $\nu \equiv$ kinematic viscosity; and $\kappa \equiv$ thermal diffusivity. The interested reader may find the discussions of natural convection in the review articles by Ostrach [10] and Churchill [11] useful.

The tank was placed outside the southern wall of a building (Fig. 1) with its symmetry axis on a north-south line. Before 10 AM, the tank was shaded by the building on the east (not visible in the photograph); however, the tank was in direct sunshine from approximately 10 AM to 6 PM. At local solar noon, the temperature difference $T_{\text{top}} - T_{\text{bottom}}$ was as large as 15 K, where T_{top} and T_{bottom} are the temperatures indicated by thermistors taped to the outside of the tank. At the same time, $T_{\text{probe}} - T_{\text{bottom}}$ was as large as 8 K. As one might expect, $T_{\text{top}} - T_{\text{probe}} << T_{\text{probe}} - T_{\text{bottom}}$. A naïve interpretation of these observations is: the density of the argon increased with depth and might be stably stratified (no convection), even though the Rayleigh number was $\sim5\times10^9$. However, the heating was asymmetric and that probably prevented stratification. Between 10 AM and 6 PM, the southern end of the tank was heated by the sun while the northern end was not heated. Furthermore, except at local solar noon, one side of the tank was heated by sunlight more than the opposite side.

During each night, the top of the tank was 0.1 K to 0.5 K cooler than the bottom of the tank; *i.e.* the tank was cooled from the upper surfaces with $4\times10^7 < Ra < 2\times10^8$. Reference [10] is a review of papers (prior to 1988) on measurements and calculations of natural convection within a horizontal, fluid-filled cylinder. Many of the reviewed papers and some more recent papers deal with either constant heat-flux or constant-temperature boundary conditions that have high symmetry. For example, Refs. [12, 13, 14] consider a horizontal cylinder that is uniformly heated on one horizontal band of the circumference and cooled on the diametrically opposite band; however, the warmer band is either beneath, or opposite to, the cooler band. In contrast, Refs. [15] and [16] consider a cylinder heated at one end and cooled at the opposite end. We speculate that the heat transfer and flow within the tank during the evenings resembles a

combination of these symmetrical situations because the southern end and western side of the tank will be warmer than the northern end and eastern side. From the literature, we expect that narrow, boundary-layer flows form and rise along the warmer surfaces and also form and descend along the cooler surfaces. Many of the literature models and measurements show that the gas in the core volume, encircled by the boundary layer flows, barely moves and has a temperature profile that increases linearly with height. If our tank had such a linear temperature profile, our results would be consistent with the calculation of Gillis *et al*. [4] that predicts that the acoustic resonance frequencies are determined only by the average gas temperature and are independent of a linear temperature gradient.

As noted above, the sun heated the tank from above with an asymmetry that varied throughout the day. We are not aware of a model calculation describing a cylindrical cavity heated asymmetrically from above. Dalal and Das modeled a 2-dimensional, rectangular cavity that was heated from above and that had one corrugated side-wall that broke the symmetry [17]. At $Ra = 10^6$ (their largest value of Ra) their cavity had convective rolls and a temperature gradient that was concentrated in a narrow band near the top-center of the cavity. If this situation occurred when our tank was in direct sunshine, it would explain why $(T_{top} - T_{probe})/(1\text{ cm}) >> (T_{top} - T_{bottom})/(50\text{ cm})$ and it might also explain why the thermal expansion correction in Eq. (5) had to be reduced by a factor of 0.6 to fit the p/f^2 data.

Acknowledgement

The authors thank Jim Glover of Graftel LLC for discussions that stimulated this work. We also thank Jim Schmidt for his participation in the early part of this work.

[1] M.R. Moldover, R.M. Gavioso, J.B. Mehl, L. Pitre, M. de Podesta, and J. T. Zhang, "Acoustic gas thermometry," Metrologia **51**, R1-R19 (2014).

[2] R.A. Ali, S.L. Garrett, J.A. Smith, and D.K. Kotter, "Thermoacoustic thermometry for nuclear reactor monitoring," IEEE J. Instrum. & Meas. **16**, 18-25 (2013).

[3] M.R. Moldover, J.W. Schmidt, K.A. Gillis, J.B. Mehl, and J.D. Wright, "Microwave determination of the volume of a pressure vessel," Meas. Sci. and Technol. **26**, 015304 (13pp) (2014).

[4] K.A. Gillis, J.B. Mehl, J.W. Schmidit, and M.R. Moldover, "'Weighing' a gas with microwave and acoustic resonances," Metrologia **52**, 337-352 (2015).

[5] A. N. Johnson, J. D. Wright, M. R. Moldover, and P. I. Espina, "Temperature characterization in the collection tank of the NIST 26 m^3 PVTt gas flow standard," Metrologia **40**, 211-16 (2003).

[6] K.A. Gillis and M.R. Moldover, "Practical determination of gas densities from the speed of sound using square-well potentials," Int. J. Thermophysics **17**, 1305-1324 (1996).

[7] E. W. Lemmon, M. O. McLinden, and M. L. Huber, "REFPROP: Reference fluid thermodynamic and transport properties," NIST Standard Reference Database 23, Version 9.1, Natl. Inst. Stand. and Tech., Boulder, CO, (2010). www.nist.gov/srd/nist23.cfm

[8] M. Greenspan and C. E. Tschiegg, "Sing-around ultrasonic velocimeter for liquids," Rev. Sci. Inst. **28**, 897-901 (1957).

[9] S. Garrett, G. W. Swift, and R. E. Packard, "Helium gas purity monitor for recovery systems," Physica **107B**, 601-602 (1981).

[10] S. Ostrach, "Natural convection in enclosures," J. Heat Transfer **110**, 1175-1190 (1988).

[11] S. W. Churchill, "Progress in the Thermal Sciences: AIChE Institute Lecture," A.I.Ch.E. Journal **46**, 1704-1722 (2000).

[12] W. R. Martini and S. W. Churchill, "Natural Convection Inside a Horizontal Cylinder", A.I.Ch.E. Journal **6**, 251-257 (1960).

[13] S. Ostrach, and R. G. Hantman, "Natural Convection Inside a Horizontal Cylinder," Chem. Engr. Comm. **9**, 213-243 (1981).

[14] S. Xin, P. Le Quéré, and O. Daube, "Natural convection in a differentially heated horizontal cylinder: Effects of Prandtl number on flow structure and instability," Phys. Fluids **9**, 1014-1033 (1997).

[15] H. Q. Yang, K. T. Yang, and J. R. Lloyd, "Three-dimensional laminar buoyant flow in a horizontal circular cylinder with differentially heated end walls at high Rayleigh numbers," Numerical Heat Transfer **14**, 429-446 (1988).

[16] S. Kimura and A. Bejan, "Experimental study of natural convection in a horizontal cylinder with different end temperatures, Int. J. Heat Mass Transfer **23**, 1117-1126 (1980).

[17] A. Dalal and M. K. Das, "Numerical study of laminar natural convection in a complicated cavity heated from top with sinusoidal temperature and cooled from other sides," Computers and Fluids **36**, 680-700 (2007).